

# Supplementary Information

S11 – Graphene PVP ink formulations. ....	2
S12 – Thermal Analysis of PVP .....	3
S13 – Rheological Measurements.....	4
S14 – DLS Stability Assays .....	5
S15 – SEM Imaging.....	6
S16 – Spray-coating repeatability .....	7
S17 – Identifying optimal $V_{GS}$ .....	8
S18 – pH Sensing Performance .....	9
S19 – $Na^+$ Selective GFET Sensing Performance.....	10
References .....	11

## SI1 – Graphene PVP ink formulations.

It is desirable for liquid phase exfoliated (LPE) inks to demonstrate high concentrations, low-flake thickness, and rheological properties adapted to the deposition method of choice.<sup>1</sup> In our work, we conducted detailed optimisation of the graphene ink production which resulted in a high concentration of 0.818 mg mL<sup>-1</sup> when centrifuged at 13000 g. Running a control centrifugation at 2300 g (which is closer to the typically used 1540 g reported in most papers in Table S1), yielded concentrations 3.1 mg mL<sup>-1</sup>, > 2.5 times higher than the previously reported highest concentrations for a graphene-PVP ink formulation.

Table S1: Table of Graphene/PVP ink formulations. All centrifugations were 1 hour long.

Formulation	Centrifugation	Concentration (mg/mL)	Reference
12 hr sonication, 10 mg mL <sup>-1</sup> Graphite in 1.5 mg mL <sup>-1</sup> PVP in IPA	1540 g	0.4	Santra et al. <sup>2</sup>
8 hr sonication, 10 mg mL <sup>-1</sup> Graphite in 0.15 mg mL <sup>-1</sup> PVP in IPA	1540 g	0.4	Koskinen et al. <sup>3</sup>
12 hr sonication, 10 mg mL <sup>-1</sup> Graphite in 0.15 mg mL <sup>-1</sup> PVP in IPA	1540 g	0.42	Dodoo-Arhinen et al. <sup>4</sup>
12 hr sonication, 10 mg mL <sup>-1</sup> Graphite in 0.25 mg mL <sup>-1</sup> PVP in IPA	1540 g	0.59	Jussila et al. <sup>5</sup>
12 hr sonication, 10 mg mL <sup>-1</sup> Graphite in 1.2 mg mL <sup>-1</sup> PVP in IPA	1540 g	0.93	Juntunen et al. <sup>6</sup>
12 hr sonication, 10 mg mL <sup>-1</sup> Graphite in 0.15 mg mL <sup>-1</sup> in 9:1 IPA:2-butanol	1540 g	1.2	Wu et al.
9 hr sonication, 50 mg mL <sup>-1</sup> Graphite in 0.4 mg mL <sup>-1</sup> PVP in IPA	<b><u>13000 g</u></b>	<b><u>0.818</u></b>	This work
9 hr sonication, 50 mg mL <sup>-1</sup> Graphite in 0.4 mg mL <sup>-1</sup> PVP in IPA	<b><u>2300 g</u></b>	<b><u>3.1</u></b>	This work

## SI2 – Thermal Analysis of PVP

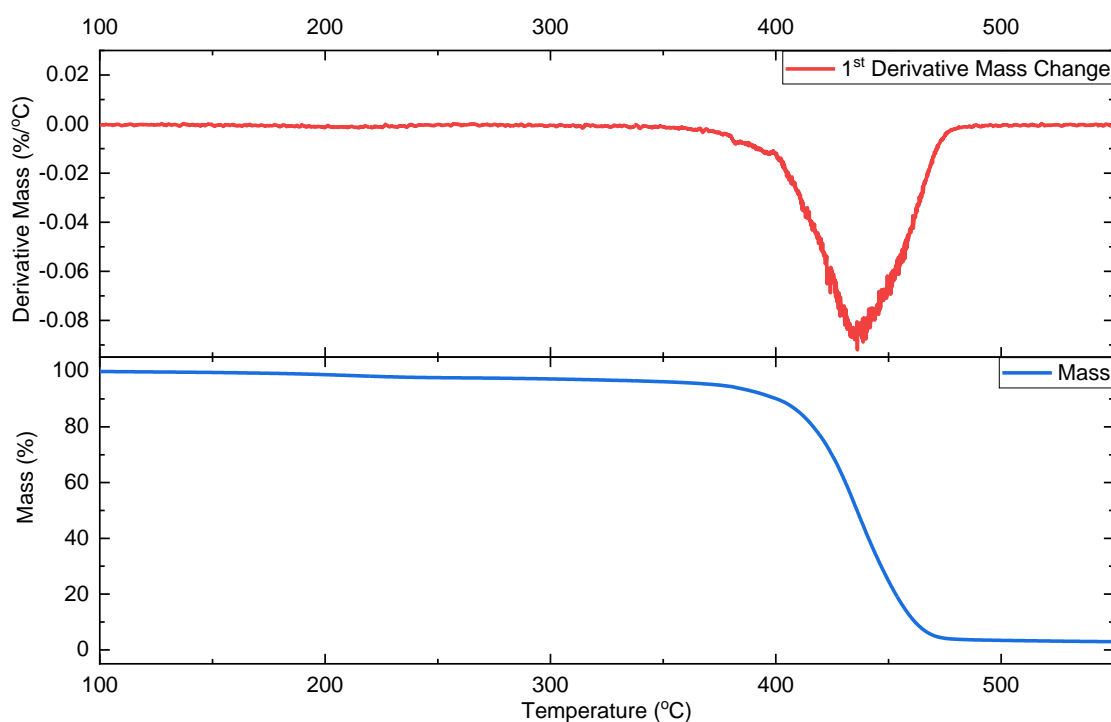


Figure S1 Thermal analysis profile, showing the decomposition of PVP as a function of temperature.

Thermogravimetry analysis (TGA) was used to determine the mass of PVP powder as a function of temperature (blue curve) up to 550 °C. 4.2708 mg was added onto a platinum crucible (Mettler Toledo). The initial decomposition temperature was 375 °C and the maximum rate of decomposition temperature was reached at 437 °C. The final residue at the end of heating was 2.91 % (0.1245 mg). Derivative thermogravimetry (DTG) was used to resolve independent components (red curve) and show a single transition in the decomposition of PVP.

### SI3 – Rheological Measurements

The graphene ink rheology was measured at 25 °C. The graphene ink rheology was tailored to be appropriate for spray coating. The graphene ink density is  $789 \text{ kg m}^{-3}$ , the surface tension was calculated to be  $18.50 \pm 0.25 \text{ mN m}^{-1}$  and viscosity is  $2.35 \text{ mPa s}$ .

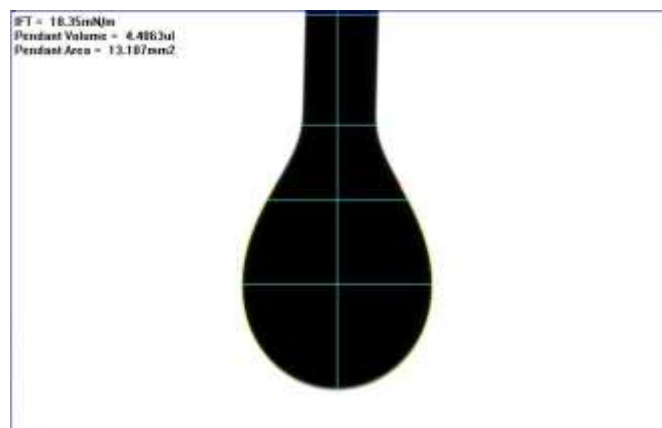


Figure S2 Interfacial tension (IFT) measurement of LPEG ink. Average IFT on 15 drops yielded an IFT of  $18.50 \pm 0.25 \text{ mN m}^{-1}$ .

## SI4 – DLS Stability Assays

DLS is an optical technique that measures the constant random Brownian motion of particles suspended in a fluid.<sup>7</sup> A coherent light source is shown on the sample and the time-dependent phase shift causing by the scattering of light by the suspended particles is recorded. The scattering signal is further processed by algorithms to give the mean particle sizes and polydispersity index.

Aliquots of the inks were separated into 1 mL Eppendorf tubes and stored under ambient conditions. Aliquots were retrieved over time and diluted for analysis. Initially, DLS measurements were conducted on a serial dilution of graphene ink to identify the concentration range at which the measured particle size is independent of dilution factor (Figure S3b). The variation in the  $Z_R$  is a result of the changing interactions of the flakes with light at different concentrations. Low particle concentrations weakly scatter light, resulting in excessive noise whereas high particle concentrations result in strong particle-particle interactions that distort the size results.<sup>8</sup> A dilution factor of 61 was identified as optimum because this fit within the range of dilution factors where the  $Z_R$  is not dependent on the dilution factor.

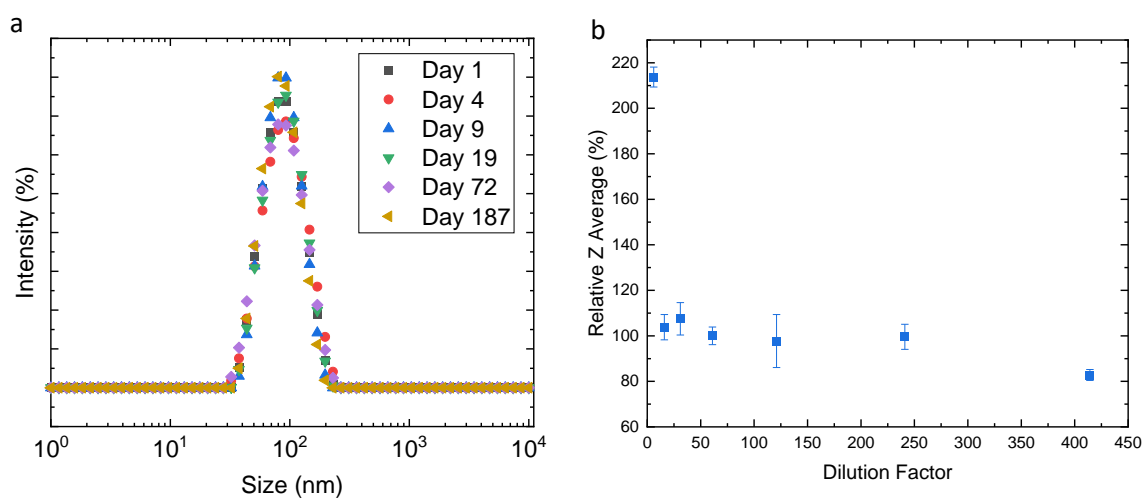


Figure S3: a) DLS intensity peak profile, showing a single monodisperse peak. The absolute size values were not used as these assume a spherical particle shape, but rather the  $Z_R$  was used in monitoring the graphene ink. b) Identification of the appropriate concentration for DLS.

## SI5 – SEM Imaging

SEM lateral flake size,  $\langle S \rangle$  distribution measurement. The fitting is log-normal with a peak at 182 nm. This corresponds closely to the measurement conducted using AFM.

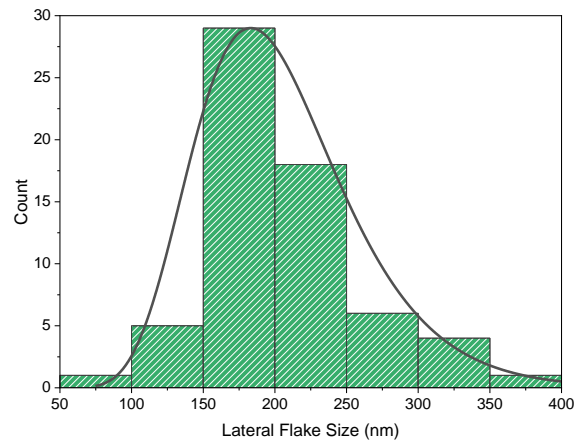
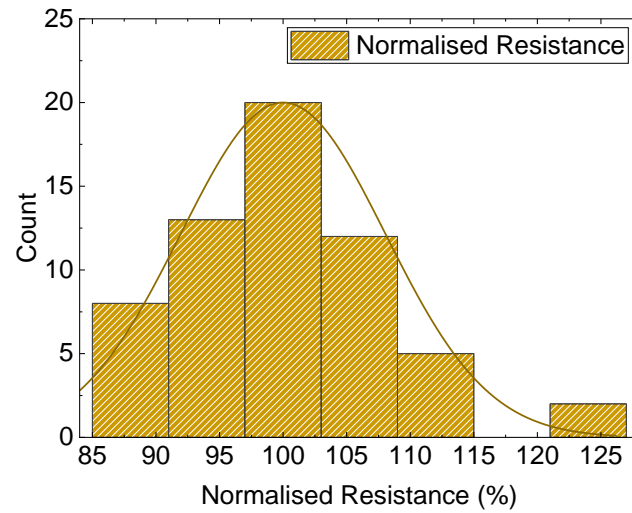


Figure S4: Flake size distribution using SEM, showing a log-linear distribution peaking at 182 nm.

## SI6 – Spray-coating repeatability

The batch repeatability statistics below (Figure S5) show the standard deviation of graphene channel electrical from the mean channel electrical resistance (=100%) is 8%. All 60 fabricated devices were functional within the range of 85% - 125% of the mean channel resistance.



*Figure S5:* Distribution of electrical resistances of graphene channels sprayed in one batch, showing the repeatability of the spray-coating process.

## SI7 – Identifying optimal $V_{GS}$

We use the  $V_{GS}$  sweeps to identify the ideal  $V_{GS}$  value for sensing. A  $V_{GS}$  value of + 50 mV was chosen for pH sensing as it is in the linear regime of the  $I_D$  response and is also the  $V_{GS}$  at which the minimum magnitude of  $I_G$  occurs (Figure S7).

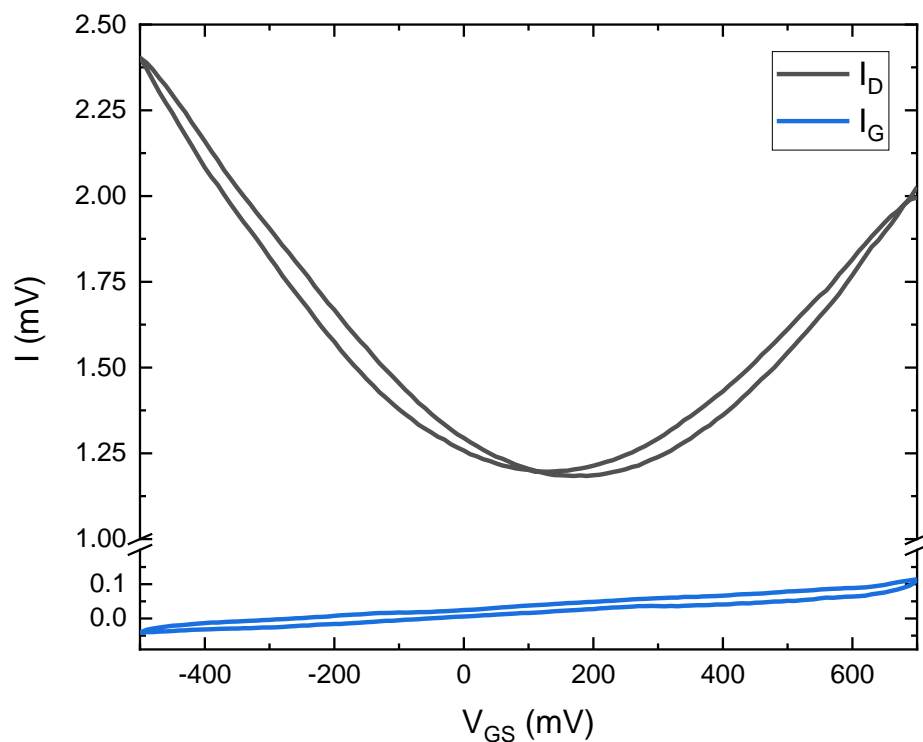


*Figure S6:*  $V_{GS}$  sweep showing the resulting  $I_D$  (black plot) and  $I_G$  (blue plot). The  $I_D$  plot shows typical ambipolar behaviour of graphene in EG-GFET, with the point of minimal current known as the Dirac point. The  $I_G$  shows a very small gate current across the range of  $V_{GS}$  which is smallest at approximately + 50 mV. The  $V_{GS}$  at minimal  $I_G$  (+50 mV) was used as the  $V_{GS}$  for the constant  $V_{GS}$  measurements.

## SI8 – pH Sensing Performance

We demonstrate the operation of multiple GFETs working with high precision for the detection of pH ( $\text{H}_3\text{O}^+/\text{OH}^-$ ). The mean resistance at 180 s is taken as the 100 % signal response, and subsequent changes in resistance are reported in proportion to it. Figure S7 shows the comparison of two GFET transistors with added stimulus (aliquots of  $\text{H}_3\text{O}^+$ ) versus their control, showing the settling and attainment of a constant  $I_D$  at approximately 180 s.

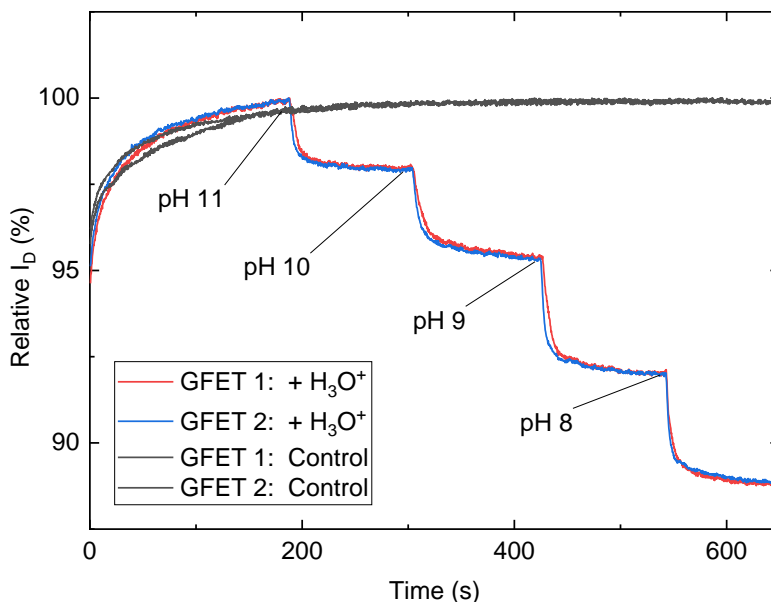


Figure S7: Comparison of  $I_D$  response of EG-GFET, with and without (control) additions of  $\text{H}_3\text{O}^+$ .

Ten EG-GFETs (from 5 separate spray coating batches) were used to detect for pH ( $N = 10$ ). The EG-GFETs show a mean sensitivity  $3.05 \pm 0.15$  % per pH unit, between pH 3 and 11, with an adjusted  $R^2 = 98.04$  %.

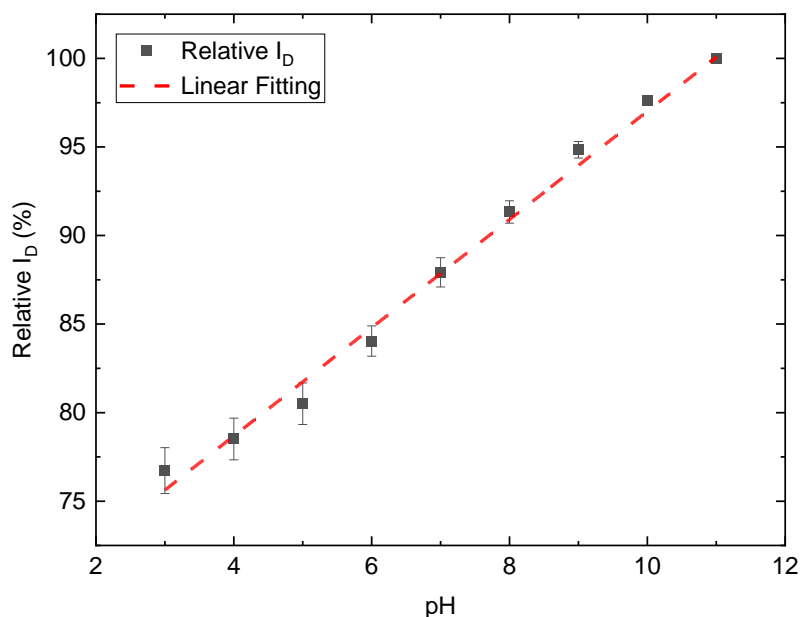


Figure S8: Relative  $I_D$  (normalised to  $I_D$  at pH 11) against pH taken at  $V_{DS} = 0.2$  and  $V_{GS} = -0.22$ . Error bars depict the standard deviation of the  $I_D$  response at that specific pH.

## SI9 – Na<sup>+</sup> Selective GFET Sensing Performance

We demonstrate the operation of multiple GFETs working with high precision for the detection of Na<sup>+</sup>. The mean resistance at 300 s is taken as the 100 % signal response, and subsequent changes in resistance are reported in proportion to it. Figure S9 shows the comparison of two GFET transistors with added stimulus (aliquots of Na<sup>+</sup>) versus their control, showing the settling and attainment of a constant  $I_D$  at approximately 300 s.

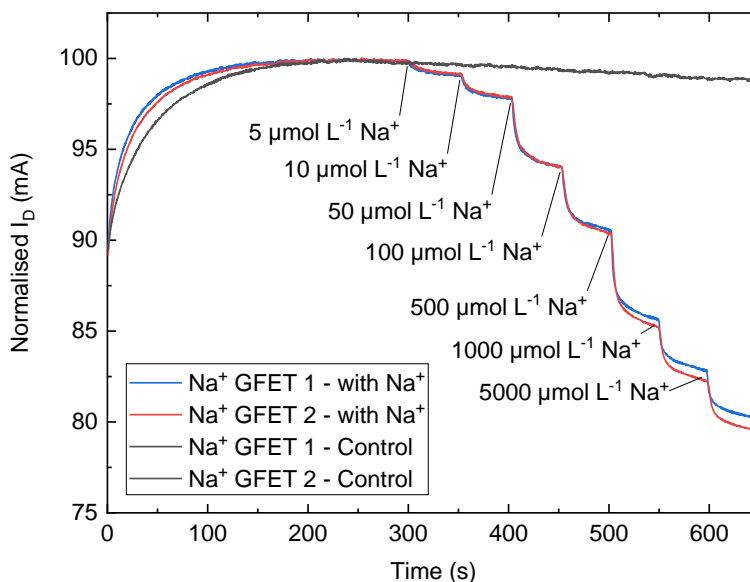


Figure S9: Comparison of  $I_D$  response of Na<sup>+</sup> GFET, with and without (control) additions of Na<sup>+</sup>.

Two Na<sup>+</sup> EG-GFETs were simultaneously used to detect for Na<sup>+</sup> for 5 times ( $N = 10$ ). Between each reading, the transistors were immersed in deionised water for 10 minutes. The EG-GFETs show a mean sensitivity of  $-6.58 \pm 0.19$  % per  $\log_{10}$  change in Na<sup>+</sup> concentration, between 5  $\mu\text{mol L}^{-1}$  and 10 mmol  $\text{L}^{-1}$ , with an adjusted  $R^2 = 99.43$  %.

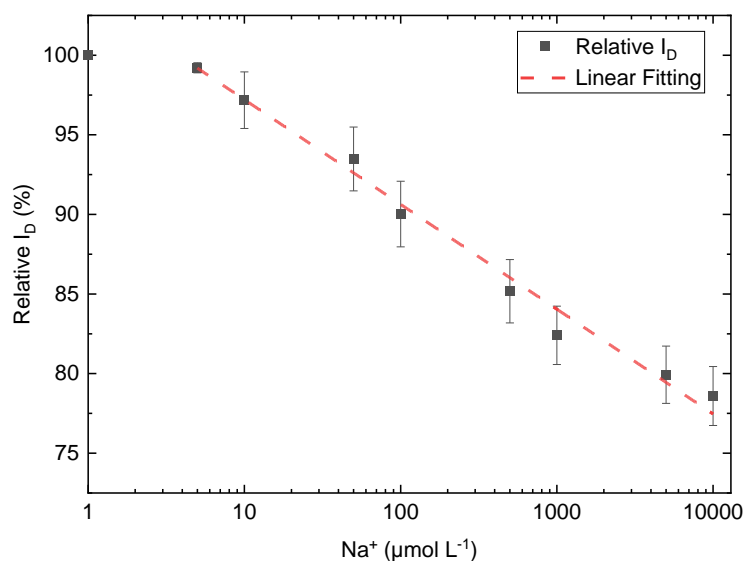


Figure S10: Relative  $I_D$  (normalised to  $I_D$  at  $\text{Na}^+ < 1 \mu\text{mol L}^{-1}$ ) against Na<sup>+</sup> concentration taken at  $V_{DS} = 0.2$  and  $V_{GS} = -0.1$ . Error bars depict the standard deviation of the  $I_D$  response at that specific Na<sup>+</sup> concentration.

## References

1. Torrisi, F. & Carey, T. *Flexible Carbon-Based Electronics* 131–205 (2018).doi:10.1002/9783527804894.ch6
2. Santra, S. et al. *Sci Rep* **5**, (2015).
3. Koskinen, T., Juntunen, T. & Tittonen, I. *Sensors (Switzerland)* **20**, 1–11 (2020).
4. Dadoo-Arhin, D. et al. *Carbon N Y* **105**, 33–41 (2016).
5. Jussila, H. et al. *ACS Omega* **2**, 2630–2638 (2017).
6. Juntunen, T. et al. *Adv Funct Mater* **28**, (2018).
7. British Standards Institute (2008).doi:10.3403/30143123
8. Berne, B.J., Wiley, J., Sons, I. & Pecora, R. (2000).